Electronic Supplementary Material (ESI) for Journal of Materials Chemistry C.

Supporting Information

Valence state regulation of iron oxide composited with graphene towards negative electrodes in asymmetric supercapacitors

Zhihao Song [a, b, c], Nian Li [a, c, *], Jun Kang [a, b, c], Liqing Chen [a, b, c], Yanping Song [a, b, c], Xinling Yu [d], Hu Ge [c, d], Zhao Li [a, b, c], Na Hong [a, b, c], Shudong Zhang [a, c, *], and Zhenyang Wang [a, c, *]

[a] Institute of Solid State Physics, Hefei Institutes of Physical Science, Chinese Academy of Sciences, Hefei, 230031, China.

[b] University of Science and Technology of China, Hefei, 230026, China.

[c] Key Laboratory of Photovoltaic and Energy Conservation Materials, Hefei Institutes of Physical Science, Chinese Academy of Sciences, Hefei, 230031, China.

[d] Hefei University, Hefei, 230601, China.

E-mail:

linian@issp.ac.cn; sdzhang@iim.ac.cn; zywang@iim.ac.cn

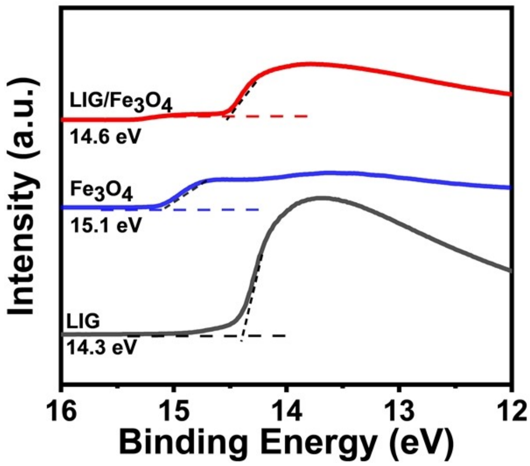

Figure S1. UPS spectra of LIG, Fe_3O_4 and LIG/Fe_3O_4.

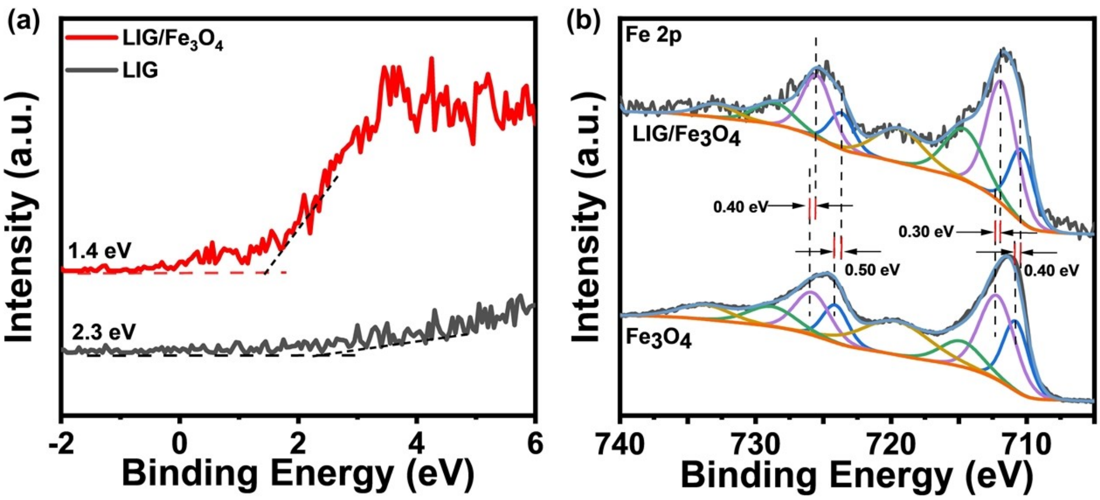

Figure S2. (a) Valence band XPS of LIG and LIG/Fe_3O_4. (b) XPS spectra of Fe2p of Fe_3O_4 and LIG/Fe_3O_4.

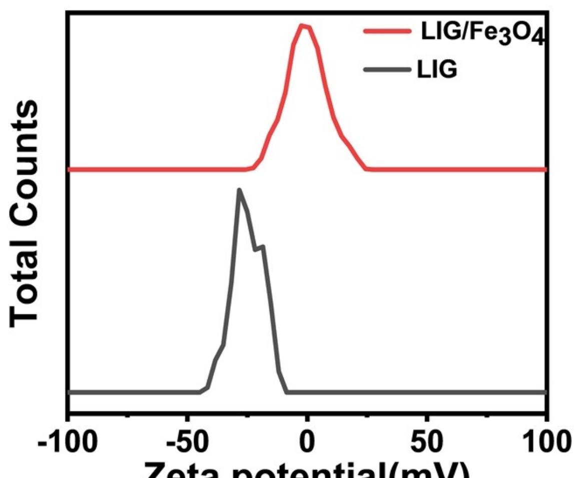

Figure S3. The zeta potential analysis of LIG and LIG/Fe_3O_4 composites.

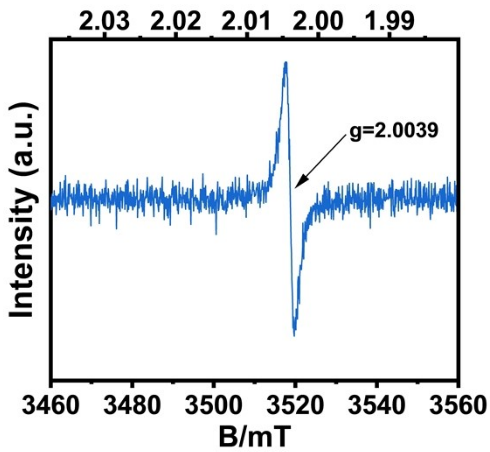

Figure S4. The EPR spectra of LF (LIG/Fe_3O_4).

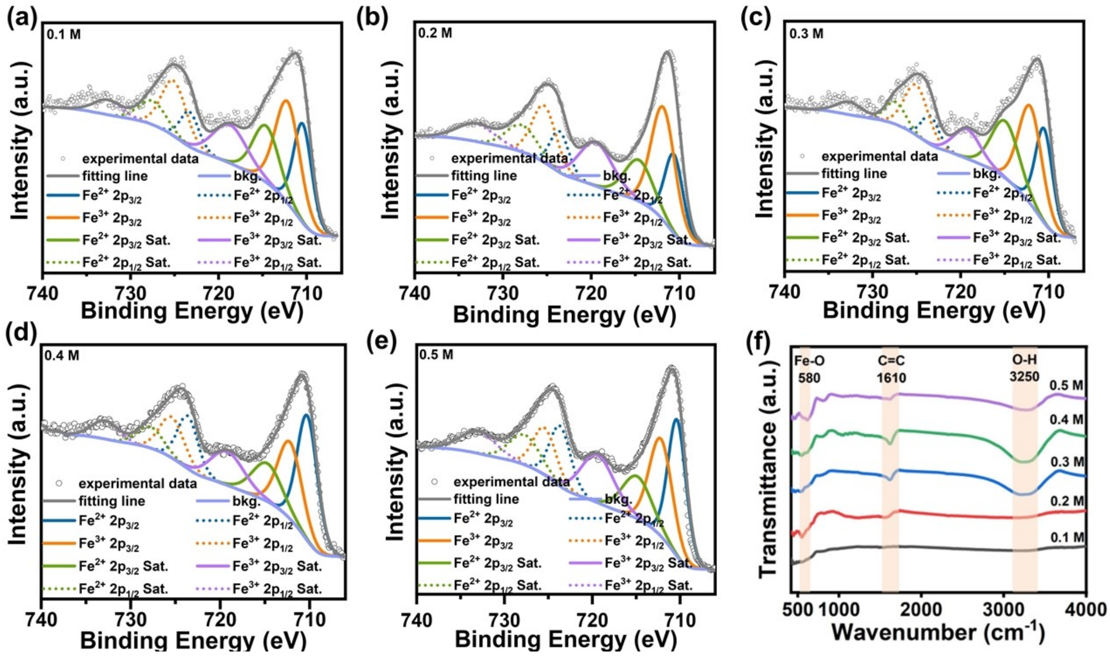

Figure S5. The Fe2p high-resolution XPS spectra of various concentrations(a-e); FTIR spectra of MF under different concentration(f).

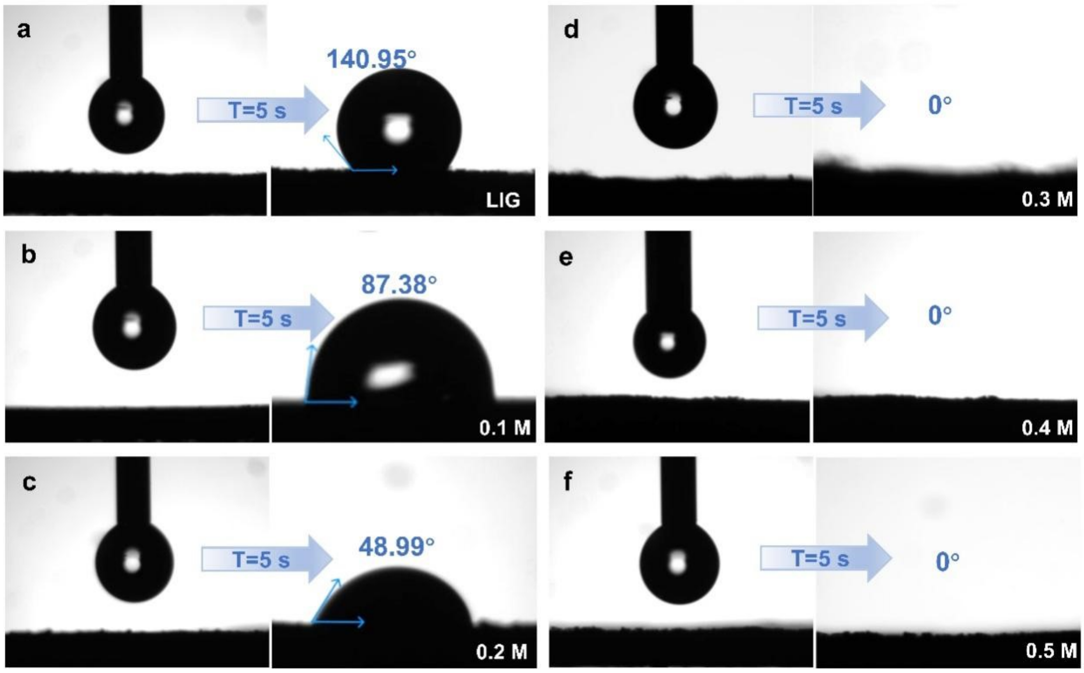

Figure S6. Contact angle testing of LIG (a) and MF (b-f) at different concentration.

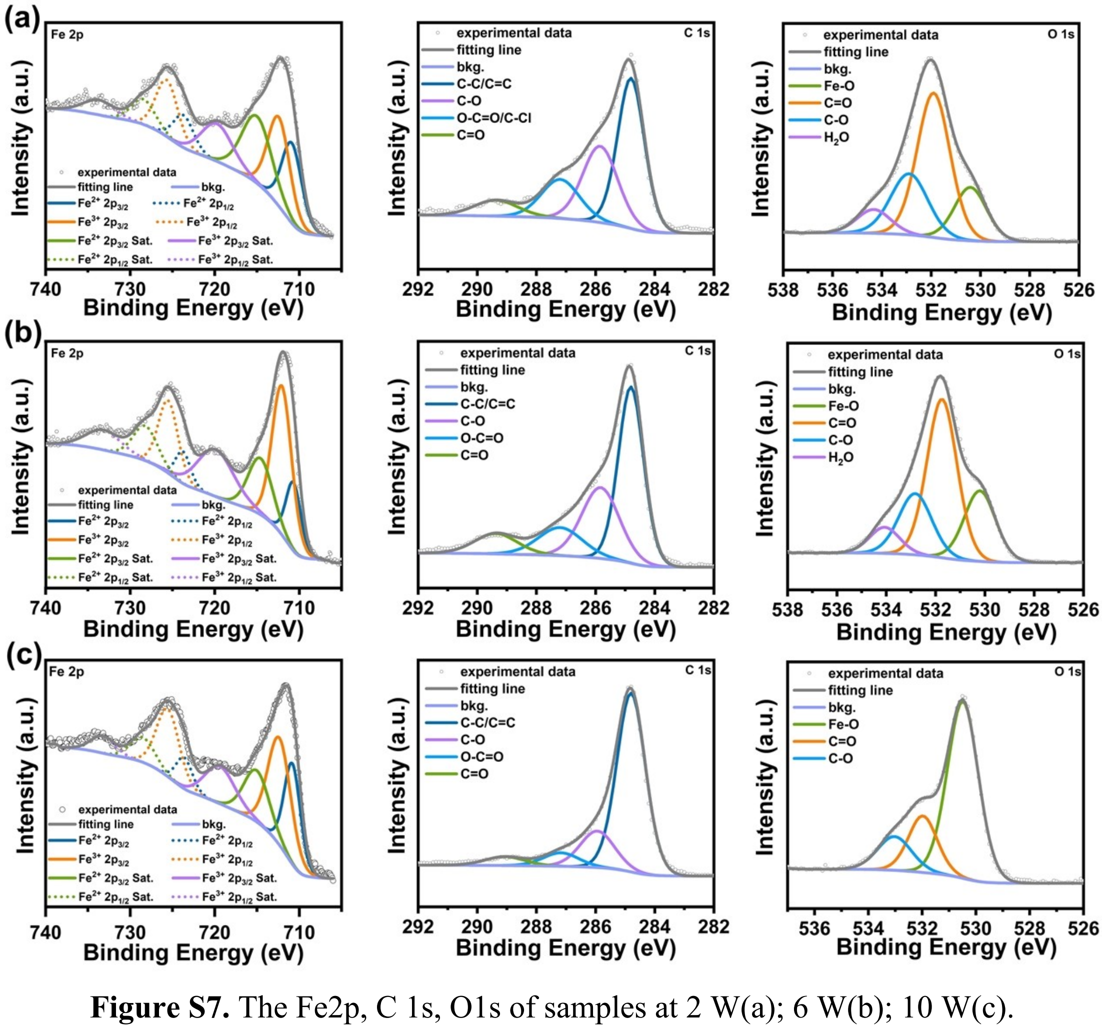

Figure S7. The Fe2p, C 1s, O1s of samples at 2 W(a); 6 W(b); 10 W(c).

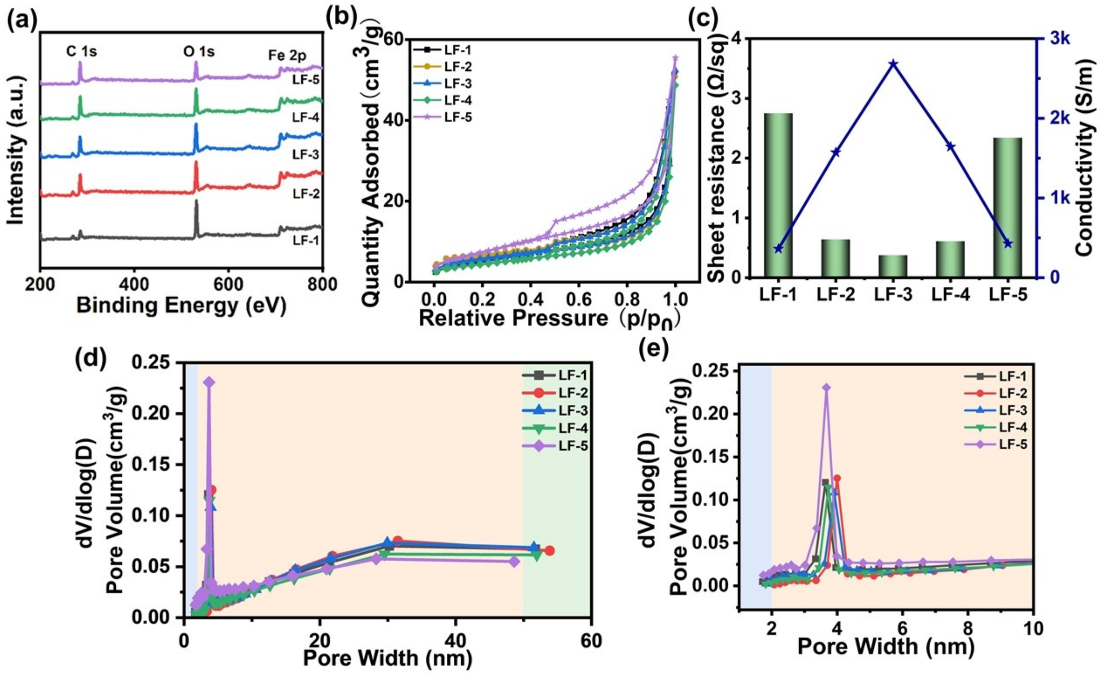

Figure S8. The full XPS spectrum of LF (a); The BET analysis results of different LF samples(b); The resistance and conductivity of different LF samples(c); The Porosity (calculated by using the DFT model) of LF and the pores of different ranges are classified and enlarged (d).

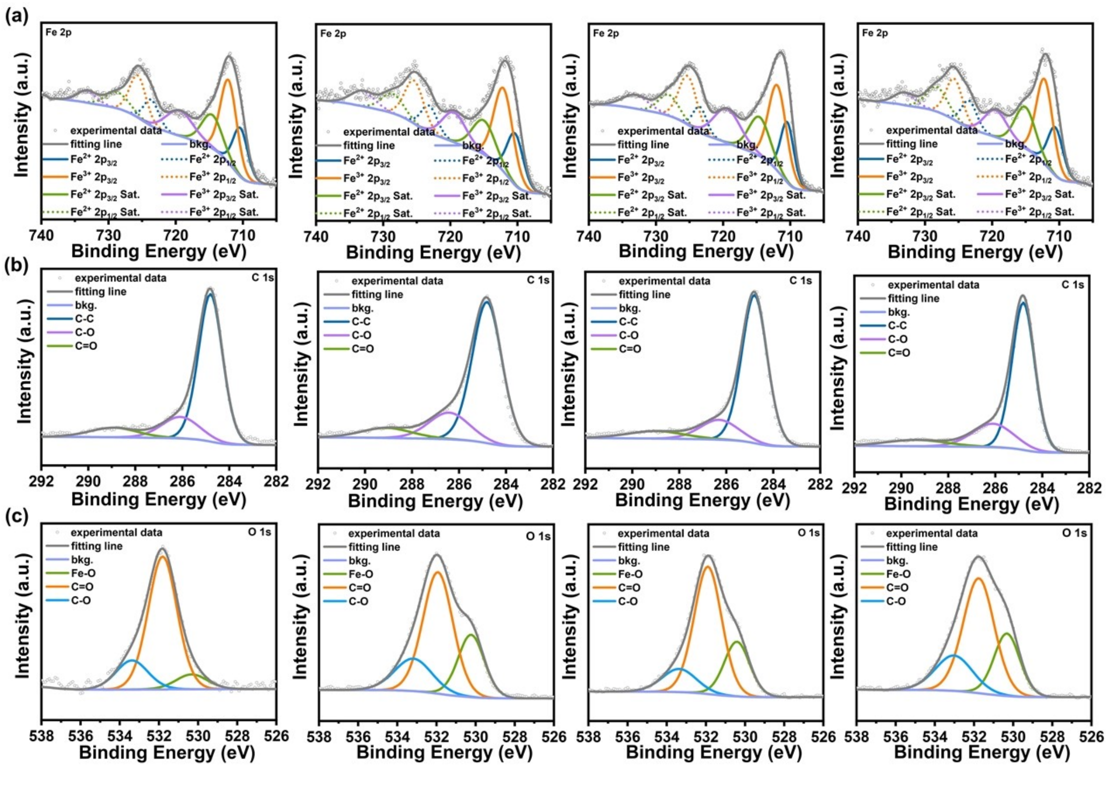

Figure S9. The Fe 2p (a), C 1s (b), O1s (c) of LF-1, LF-2, LF-4, LF-5.

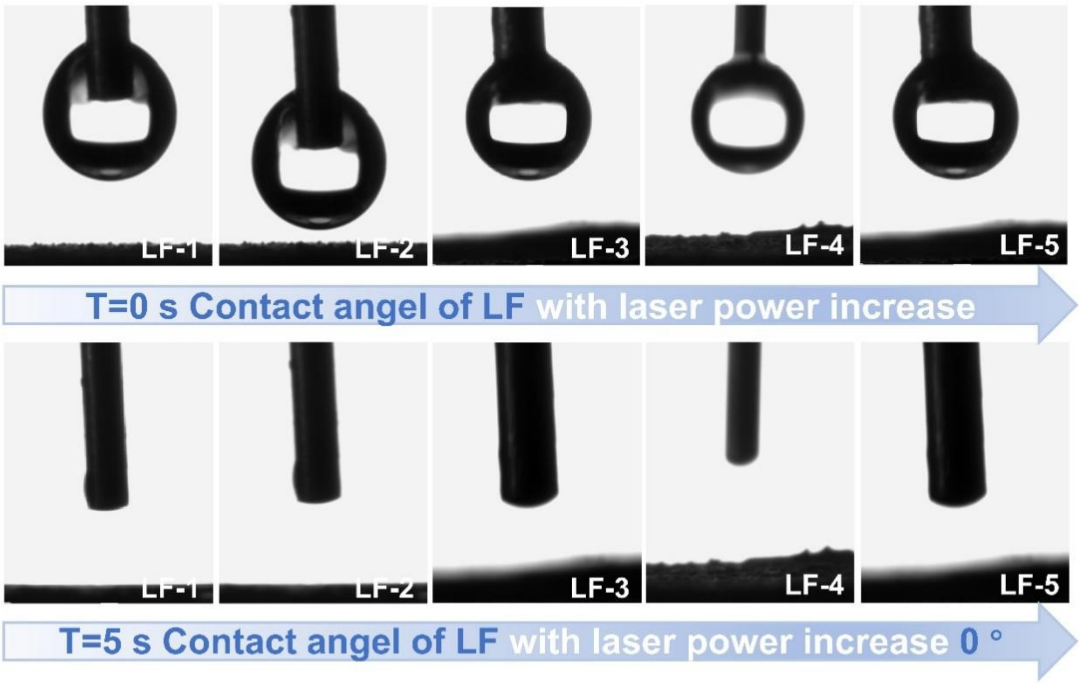

Figure S10. Contact angle testing of LF at different laser power.

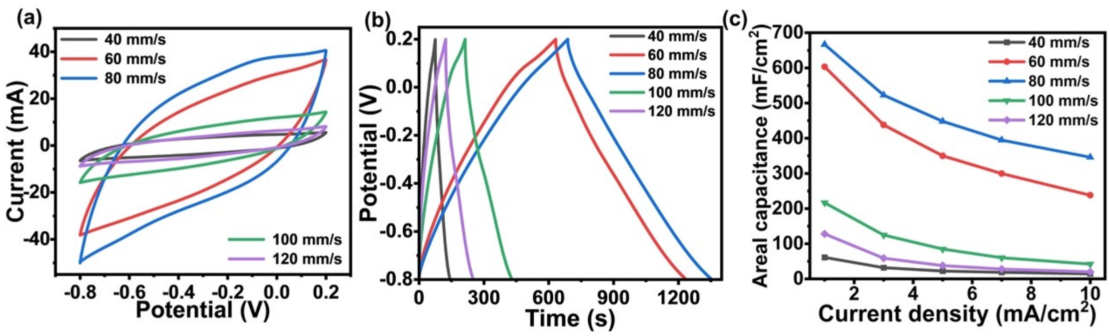

Figure S11. (a)The CV curves at the voltage scanning rates of 100 mV/s; (b) The GCD diagrams at 1mA/cm^2 ;(c) Areal capacitance of different laser scanning rate.

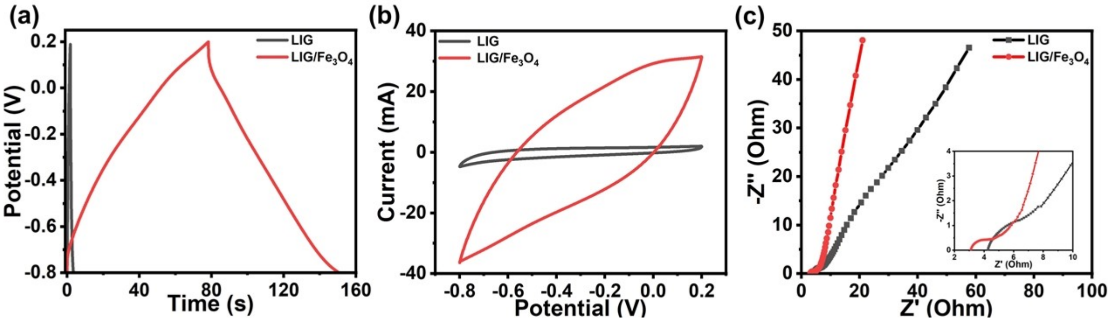

Figure S12. Comparison of (a)The CV curves; (b) The GCD diagram ;(c) The Nyquist curves between LIG and LF.

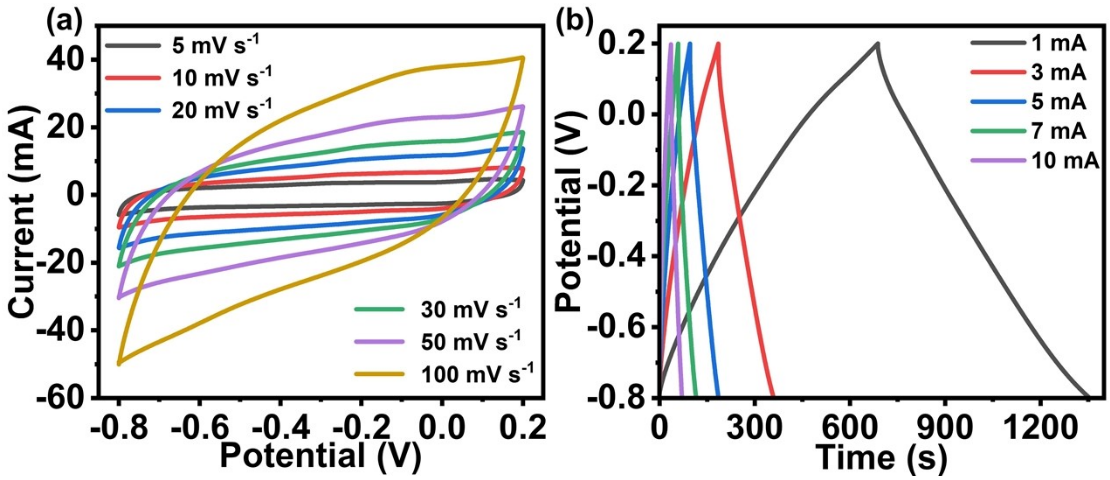

Figure S13. (a) The CV curves of the LF-3. (b) The GCD curves of the LF-3.

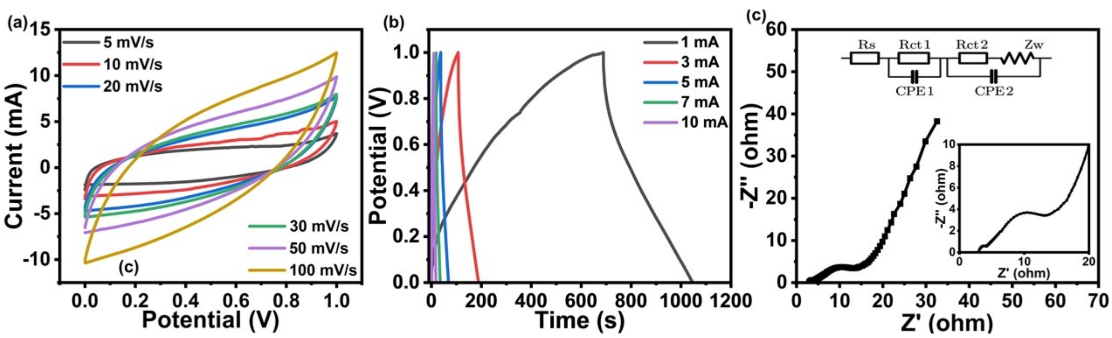

Figure S14. The CV (a), GCD (b) and (c) EIS curves of the AC.

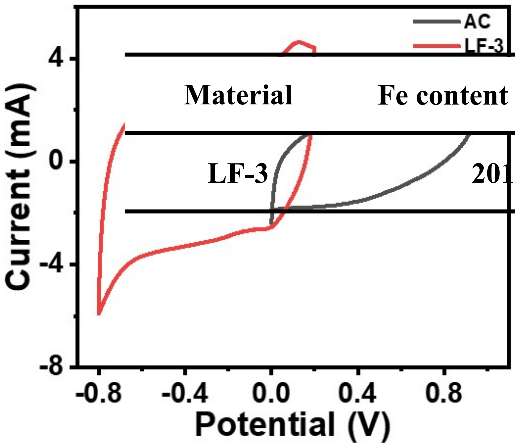

Figure S15. Comparison of the CV curves at 5 mV/s between AC and LF-3.

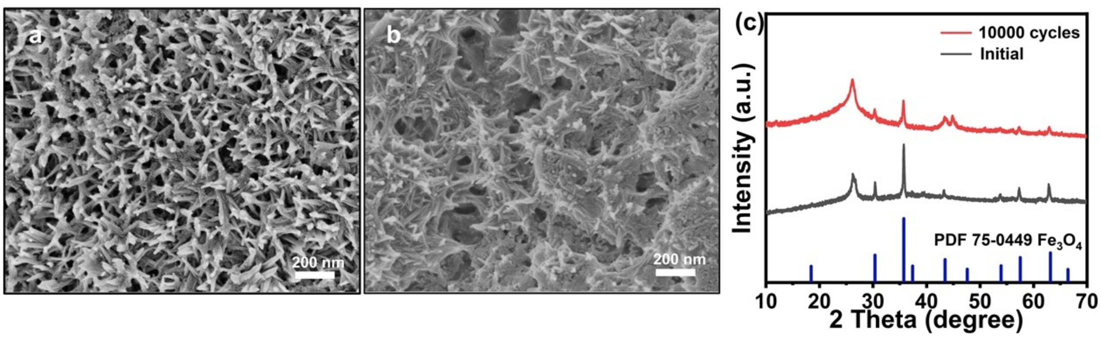

Figure S16. SEM image of LF-3 initially (a) and after 10000 cycles (b). (c)XRD image of LF-3 initially and after 10000 cycles.

Table S1 Content of Fe and Fe_3O_4 in LF-3 by inductively coupled plasma test (ICP).

Material	Fe content（mg/g)	Fe_3O_4 content（mg/g)
LF-3	201	278.3

Table S2 Comparison of voltage ranges for different negative electrode materials**.**

Material	Voltage	Ref
Mxene/Fe_3O_4/MXene	**-0.7-0 V**	**72**
Fe_3O_4 /MXene/RGO	**-1-0 V**	**78**
NCSs@Fe_3O_4	**-1-0 V**	**79**
Fe_3O_4@3DGr	**-1-0 V**	**80**
Fe_3O_4 NSs@ERGO	**-1.1-0 V**	**81**
Fe_3O_4@C	**-1- -0.15 V**	**82**
Fe_3O_4@PANI	**-0.8-0.2 V**	**83**
LF	**-0.8-0.2 V**	**This work**

Table S3 Impedance parameters derived using equivalent circuit model for the LF.

Material	R_s (Ω)	R_{ct} (Ω)	Z_w (Ω)
LF-1	**3.19**	**5.91**	**8.24**
LF-2	**3.15**	**4.40**	**6.10**
LF-3	**2.96**	**1.38**	**1.53**
LF-4	**3.08**	**2.46**	**2.93**
LF-5	**3.53**	**6.26**	**6.28**

Table S4 Comparison

of the areal capacitance with various Fe_3O_4 material.

LIG/Fe_3O_4	**0-1 V**	**43.6 (1mA/cm^2)**	**71**
Mxene/Fe_3O_4/MXene	**0-0.7 V**	**46.4 (0.5 mA/cm^2)**	**72**
C- Fe_3O_4/PLA	**0-2 V**	**47.9 (1 mA/cm^2)**	**73**
Fe_3O_4-FMWCNT	**0-2 V**	**78.5 (1 mA/cm^2)**	**74**
LF	**0-1.5 V**	**106.4 (1 mA/cm^2)**	**This work**

Material	Coulombic efficiency	Ref (supplemental)
PPy/Fe_2O_3/rGO	**93.0%**	**1**
Fe_2O_3/graphene aerogel	**90.0%**	**2**
ATA–Fe_3O_4/rGO	**86.0%**	**3**
3D Fe_3O_4/rGO	**91.4%**	**4**
graphene/Fe_2O_3	**92.1%**	**5**
Fe_3O_4/Fe-CNTs	**82.1%**	**6**
Fe_3O_4–NC	**97%**	**7**
rGO-Fe_3O_4-MWCNT	**94%**	**8**
N-graphene/Fe_3O_4	**95%**	**9**
GO/Fe_3O_4 NCs	**91%**	**10**
LF	**Nearly 100%**	**This work**

Table S5 Comparison of the cycle stability, energy density and coulombic efficiency with various SC.

Material	Cycle stability	Energy density (uWh/cm^2)	Coulombic efficiency	Ref
LIG/Fe_3O_4	**74% (900)**	**60.20 (1mA/cm^2)**	**90.2%**	**71**
Mxene/Fe_3O_4/MXene	**91.7% (2000)**	**0.970 (0.5 mA/cm^2)**	**nearly 100%**	**72**
CF- Fe_3O_4	**86.1% (10000)**	**5 (1 mA/cm^2)**	**88.8%**	**75**
LIG/TiO_2/LIG	**100% (10000)**	**3.07 (0.05 mA/cm^2)**	**/**	**76**
LIG	**95% (6000)**	**4.27 (0.5 mA/cm^2)**	**87.5%**	**77**
LF	**86.8% (10000)**	**33.25 (1 mA/cm^2)**	**nearly100%**	**This work**

Table S6 Comparison of the coulombic efficiency with various SC.

References (Supplemental files):

1 A. Moyseowicz, A. Śliwak, E. Miniach and G. Gryglewicz, *Compos. B Eng.,* 2017, **109**, 23-29.

2 A. M. Khattak, H. Yin, Z. A. Ghazi, B. Liang, A. Iqbal, N. A. Khan and Z. Tang, *RSC adv*, 2016, 6, 58994-59000.

3 G. Bhattacharya, G. Kandasamy, N Soin, R. K. Upadhya, S. Deshmukh, D. Maity, J. McLaughlin and S. S. Roy, *RSC Adv.,* 2017, **7**, 327-335.

4 R. Kumar, R. K. Singh, R. A. Vaz, R.Savu and A. S. Moshkalev, *ACS Appl. Mater. Interfaces,* 2017, **9**, 8880-8890.

5 S. Guo, Z. Lou, L. Li, Z. Chen, X. Ma and G. Shen, *Nano Res.,* 2016, **9**, 424-434.

6 J. Sun, P. Zan, X. Yang, L. Ye and L. Zhao, *Electrochim. Acta*, 2016, **215**, 483-491.

7 J. Zhou, C. Zhang, T. Niu, R. Huang, S. Li, J. Zhang and J. G. Chen, *ACS Appl. Energy Mater.,* 2018, **1**, 4599-465.

8 S. Ranmanathan, M. Sasikumar, N. Radhika, A. Obadih, A. Durairaj, G.Swetha, P. Santhoshkumar, I. Lydia and S. Vasanthkumar, *Mater. Today: Proc.,* 2021, **47**, 843-852.

9 L. Li, Y. Dou, L. Wang, M. Luo and J. Liang, *RSC adv,* 2014, **4**, 25658-25665.

10 H. Ragupathi, J. Mariadhs, K. Venkatesh and S. S. R. Inbaanathean, *Colloids Surf. A Physicochem. Eng. Asp.,* 2024, **683**, 132927.

11 L. Chen, C. Shi, X. Li, Z. Mi, D. Wang, H. Liu and L. Qiao, *Materials,* 2017, **10**, 273.

12 Z. He, Y. Wang, Y. Li, J. Ma, Y. Song, X. Wang and F. Wang, *J Alloy Compd.,* 2022, **899**, 163241.

13 L. Canil, T. Cramer, B. Fraboni, D. Ricciarelli, D. Meggiolaro, A. Singh and A. Abate, *Energy Environ. Sci.*, 2021, **14**, 1429-1438.

14 S. K. Kumar, D. Pandey and J. Thomsa, *ACS Energy Lett.*, 2021, **6**, 3590-3599.

15 Z. Liu, W. Gao, L. Liu, S. Luo, C. Zhang, T. Yue and J. Wan and J. Hazard, *Mater.*, 2023, **442**, 130036.

16 P. Xia, S. Cao, B. Zhu, M. Liu, M. Shi, J. Yu and Y. Zhang, *Angew. Chem. Int. Ed.,* 2020, **59**, 5218-5225.

17 H. Y. Zhang, L. X. Li, W. J. Sun, J. H. He, Q. F. Xu and J. M. Lu, *ChemElectroChem*,

2023, **10**, 1-7.

18 M. Hassan, K. R. Reddy, E. Haque, S. N. Faisal, S. Ghasemi, A. I. Minett and V. G. Gomes, *Compos Sci Technol, 2014, **98**, 1-8.*

19 M. N. El-Shafai, S.M. Ramodan, A. A. Alayyafi, S. Y.Mostafa and I. El-Mehasseb, *J. Energy Storage,* 2024, **76**, 109727.

20 A. M. Navarro-Suárez, K. Maleski, T. Makaryan, J. Yan, B. Anasori and Y. Gogotsi, *Batteries Supercaps*, 2018, **1**, 33-38.

21 Z. Wei, Y. Liu, J. Wang, R. Zong, W. Yao, J. Wang and Y. Zhu, *Nanoscale,* 2015, **7**, 13943 –13950.

22 J. J. Li, B. Weng, S. C. Cai, J. Chen, H. P. Jia, Y. J. Xu and J. Hazard, *Mater,* 2018, **342**, 661–669.

23 W. Zhen, W. Wang, W. Li, X. Bai, J. Zhao, E. C. M. Tse, D. L. Phillips and Y. Zhu, *Angew. Chem. Int. Ed,* 2021, **60**, 8236-8242.